

Photogeneration of α -Bimetalloid Radicals via Selective Activation of Multifunctional C1 Units

Lewis McGhie, Alessandro Marotta, Patrick O. Loftus, Peter H. Seeberger, Ignacio Funes-Ardoiz,* and John J. Molloy*



Cite This: *J. Am. Chem. Soc.* 2024, 146, 15850–15859



Read Online

ACCESS |



Metrics & More

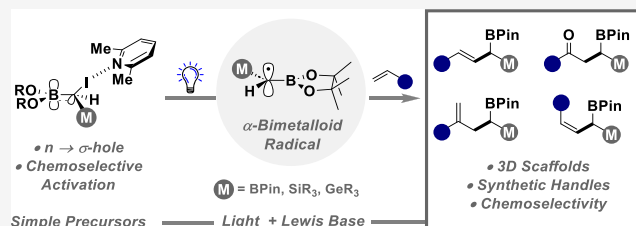


Article Recommendations



Supporting Information

ABSTRACT: Light-driven strategies that enable the chemoselective activation of a specific bond in multifunctional systems are comparatively underexplored in comparison to transition-metal-based technologies, yet desirable when considering the controlled exploration of chemical space. With the current drive to discover next-generation therapeutics, reaction design that enables the strategic incorporation of an sp^3 carbon center, containing multiple synthetic handles for the subsequent exploration of chemical space would be highly enabling. Here, we describe the photoactivation of ambiphilic C1 units to generate α -bimetalloid radicals using only a Lewis base and light source to directly activate the C–I bond. Interception of these transient radicals with various SOMOPhiles enables the rapid synthesis of organic scaffolds containing synthetic handles (B, Si, and Ge) for subsequent orthogonal activation. In-depth theoretical and mechanistic studies reveal the prominent role of 2,6-lutidine in forming a photoactive charge transfer complex and in stabilizing *in situ* generated iodine radicals, as well as the influential role of the boron p-orbital in the activation/weakening of the C–I bond. This simple and efficient methodology enabled expedient access to functionalized 3D frameworks that can be further derivatized using available technologies for C–B and C–Si bond activation.



INTRODUCTION

The rational design and construction of molecules that target a specific biological function remain a core construct in the discovery of next-generation therapeutics.¹ In contemporary medicinal chemistry, there is an overwhelming reliance on synthetic tools that facilitate the rapid and efficient exploration of chemical space in a strategically controlled manner.² In this regard, palladium-catalyzed cross-coupling reactions have been revolutionary, where preinstalled metals/metalloids or (pseudo)halides are leveraged as sp^2 exit vectors enabling the efficient extension into 2D chemical space (Figure 1A).³ The translation to multifunctional platforms has seen the inception of chemoselective activation strategies, exploiting differences in bond dissociation energy for oxidative addition ($I > Br \geq OTf > Cl$),⁴ and orthogonal reactivity of pendant nucleophiles for selective engagement in transmetalation (B vs Si vs Ge).⁵ The utility of boron-protecting groups has further expanded this concept to the iterative and automated synthesis of complex molecules,^{6,7} and given this impact, it serves as no great surprise that an estimated greater than 40% of all C–C bond formations in medicinal chemistry are currently achieved via the Suzuki–Miyaura cross-coupling reaction.⁸

Given the current drive to “escape from flatland” in the design of novel pharmaceuticals,⁹ multifunctional sp^3 systems where the described orthogonal reactivity could be emulated would be highly enabling when considering the synthesis of

molecules that occupy 3D chemical space (Figure 1B). However, while selective functionalization of a multifunctional C1 unit is desirable, moving from positionally distinct synthetic handles (sp^2) to unifying them on a single atom (sp^3) coincides with constraints on intrinsic reactivity due to a direct influence on electronic and steric parameters.¹⁰

Classic solutions to overcome this obstacle include deprotonation and harnessing reactive organometallics to generate α -bimetalloid anion synthetic equivalents (Figure 1C).¹¹ These reactive intermediates are still frequently employed and have been leveraged in elegant strategies for mono- or chemoselective activation ($M = \text{Li}, \text{B}, \text{Si}$) enabling efficient reactivity with various electrophiles,¹² and application in transition metal-catalyzed cross-coupling.¹³ The recent emergence of trivalent ambiphilic C1 units that contain at least one pendant C–X bond has enabled extension to α -bimetalloid electrophile synthetic equivalents (Figure 1C),¹⁴ where selective engagement of the C–X bond is achieved via exposure to nucleophilic species such as amines, and

Received: February 14, 2024

Revised: May 12, 2024

Accepted: May 14, 2024

Published: May 28, 2024



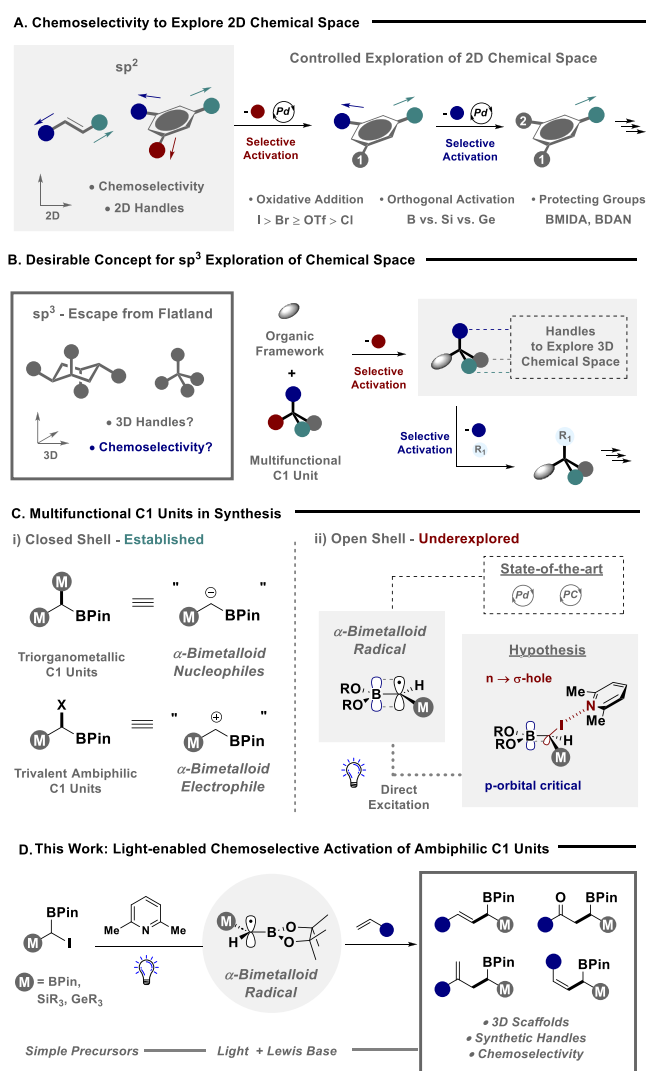


Figure 1. (A) Chemoselective exploration of 2D chemical space using Pd catalysis. (B) Concept to explore 3D chemical space. (C) Multifunctional C1 units in synthesis. (D) Light-enabled generation of α -bimetalloid radicals.

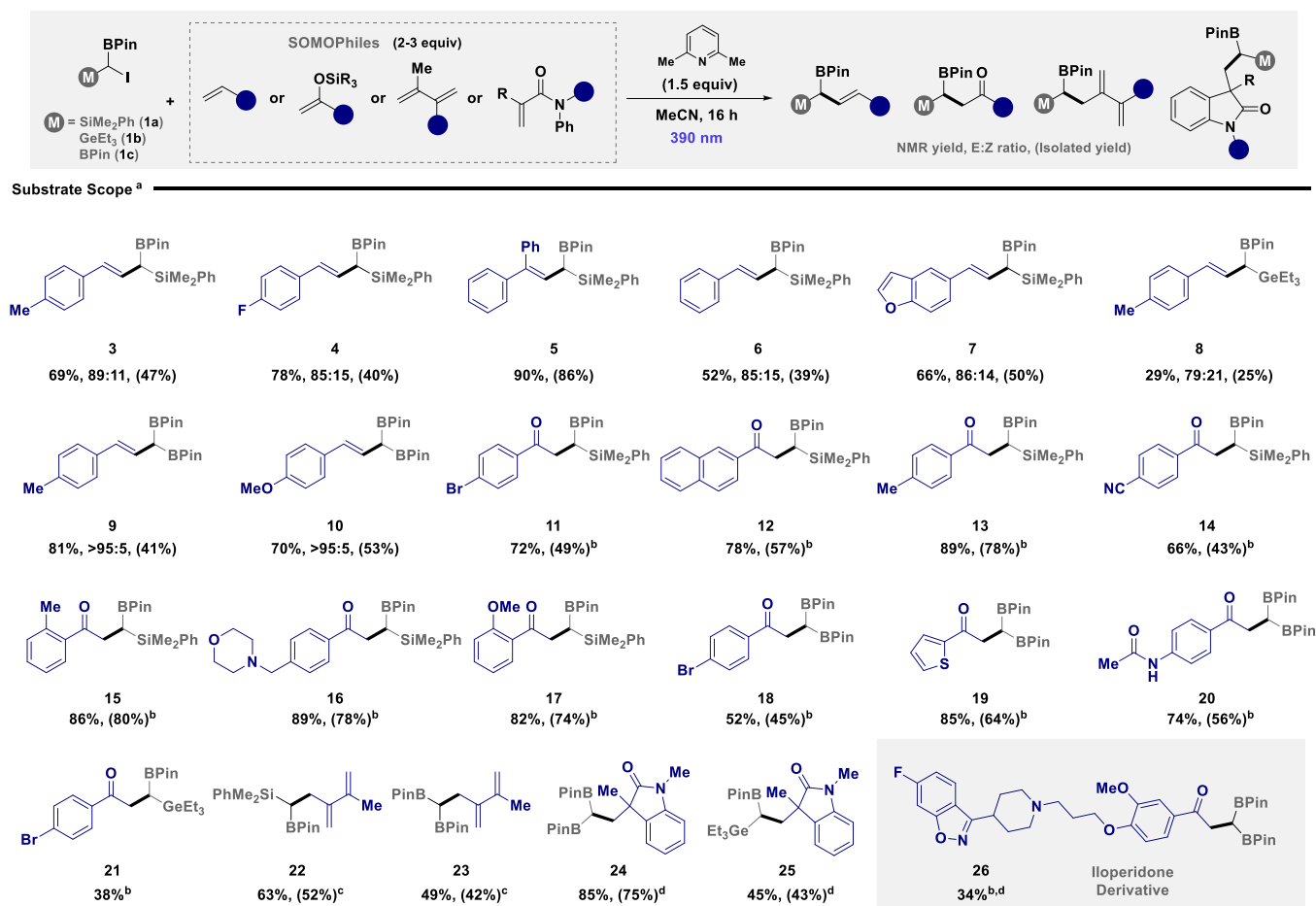
organometallics.^{14a,15} However, while closed shell reactivity has been comparatively well established and continues to expand, synthetic tools that enable the efficient generation of an α -bimetalloid radical are conspicuously underexplored, yet desirable given their orthogonal reactivity to closed shell paradigms. The current state of the art requires palladium and light as a prerequisite for efficient selective activation,^{14a,c} or photoredox catalysts to grant expedient access to cyclopropyl scaffolds.¹⁶ Motivated by the untapped potential of boron hybridization on photochemical processes,¹⁷ we envisaged that trivalent ambiphilic C1 units, containing a trigonal planar boron moiety,^{18,19} could serve as potent precursors for the operationally simple, light-enabled generation of α -bimetalloid radicals, providing a complementary approach to existing organometallic and transition metal technologies (Figure 1C, right). Here, it was anticipated that the boron p-orbital could modulate electron density at the C–I bond, resulting in a buildup of positive charge in the σ -hole of the iodine atom and ultimately a weakening of the bond. This bond could then be selectively targeted using a Lewis basic additive to generate a halogen bonding charge transfer complex that can absorb light.^{20,21} Absorption of a photon would facilitate the selective photoinduced homolytic cleavage of the C–I bond in the presence of metalloids (B, Si, Ge) that are commonly cleaved via photoactivation.^{14a,22} This would then generate an iodine radical stabilized by the Lewis base,^{23,24} and an α -bimetalloid radical primed for subsequent reactivity.

Herein, we describe the operationally simple in situ generation of α -bimetalloid radicals from easily accessible ambiphilic precursors using only light and a simple 2,6-lutidine additive (Figure 1D). Interception of these transient radicals with a series of SOMOphiles enables the rapid construction of versatile frameworks that contain multiple synthetic handles (B, Si, Ge) for the subsequent exploration of the 3D chemical space. In-depth mechanistic and computational studies unveil the importance of both the boron p-orbital and Lewis base for efficient reactivity, with the Lewis base serving a dual role in both photoactivation of the C–I bond via halogen bonding and stabilization of the iodine radical. The mild, catalyst-free protocol could be strategically paired with energy transfer catalysis to grant unprecedented access to Z-isomers containing two functional handles, rendering the process

Table 1. Optimization of Reaction Conditions^a

entry	λ (nm) ^b	solvent	additive	yield (%)	E:Z ^c
1	370	MeCN	2,6-lutidine	37	86:14
2	390	MeCN	2,6-lutidine	69	89:11
3	427	MeCN	2,6-lutidine	43	86:14
4	390	MeCN	Et ₃ N	0	n.d.
5	390	MeCN	pyridine	28	79:21
6	390	MeCN	PPh ₃	20	>95:5
7	390	MeCN	2,6-dimethyl-4-(dimethylamino)pyridine	46	74:26
8	390	THF	2,6-lutidine	3	n.d.
9	390	DMF	2,6-lutidine	0	n.d.
10	390	MeCN	2,6-lutidine	0	n.d.
11	390	MeCN	2,6-lutidine	0	n.d.

^aStandard conditions: **1a** (0.2 mmol), **2** (3 equiv), additive (1.5 equiv), solvent (0.05 M), rt 16 h. ^bReactions run using Kessil lamps 40 W. ^cDetermined by ¹H NMR spectroscopy against a known internal standard (1,3,5-trimethoxybenzene).

Scheme 1. Establishing the Substrate Scope^a

^a(a) Reactions were performed in MeCN on a 0.2 mmol scale using **1** (1 equiv), SOMOPhile (3 equiv), and 2,6-lutidine (1.5 equiv) under 390 nm irradiation (40 W). NMR yield and *E:Z* ratio were determined by ¹H NMR spectroscopy against a known internal standard (1,3,5-trimethoxybenzene). (b) 20 equiv of water was added. (c) 427 nm light was used for 48 h. (d) 2 equiv of SOMOPhile was used.

stereodivergent. The power of the overall construct for the efficient exploration of chemical space was demonstrated by product derivatization via the chemoselective activation of specific synthetic handles.

RESULTS AND DISCUSSION

We commenced our reaction optimization by investigating the efficiency of radical generation using substrate **1a**, containing both boron and silicon handles, in the presence of styrene **2** and a Lewis basic additive (Table 1). Implementing 2,6-lutidine as an additive under 370 nm (Kessil, 40 W) light irradiation afforded the allylic product *E*-**3** in an appreciable yield and selectivity (entry 1). The use of lower energy photons was beneficial using 390 nm, suppressing competitive degradation (entry 2). However, conversion to product was unsatisfactory when employing 427 nm irradiation (entry 3).

The use of alternative Lewis basic additives such as triethylamine, pyridine, and triphenylphosphine identified that 2,6-lutidine was required for efficient reactivity (entries 4–6). Increasing electron density on the Lewis base backbone was found to be detrimental to reactivity and selectivity (entry 7), while the reaction was also found to be suppressed in Lewis basic solvents (entries 8 and 9). These preliminary reactions indicate that intricate control of steric parameters and Lewis basicity of both the additive and reaction media is critical to

mitigate undesired polar reactivity with the boron p-orbital (for a comprehensive list of trialed Lewis basic additives, please see ESI for full details).²⁵ Control reactions highlight that both additive and light are required for efficient reactivity (entries 10 and 11). It is pertinent to note in both control reactions close to full recovery of substrate **1a** was achieved, indicating that both light and Lewis base are required for efficient activation of the C–I bond and that the developed method is orthogonal to ground-state reactivity previously established in the literature (Figure 1c).^{11–15}

With efficient radical generation and a general set of reaction conditions established, the scope and compatibility of the developed protocol were assessed for a series of diverse SOMOPhiles (Scheme 1). Ambiphilic reagent **1a** was efficiently coupled with styrene SOMOPhiles to afford synthetically versatile *E*-allylic products containing a pendant boron and silicon handle, in appreciable yield and good selectivity (3–7). Translation to ambiphilic reagent **1b**,^{14a} was comparatively unsuccessful (8), due to *in situ* degradation of the highly reactive allylic product under model reaction conditions. Pleasingly, ambiphilic reagent **1c**, containing *geminal*-BPIn substituents, was amenable to the protocol, enabling the rapid construction of *E*-allylic boronic esters in good selectivity (9 and 10). With a slight modification of the model reaction conditions, silyl enol ethers could also be

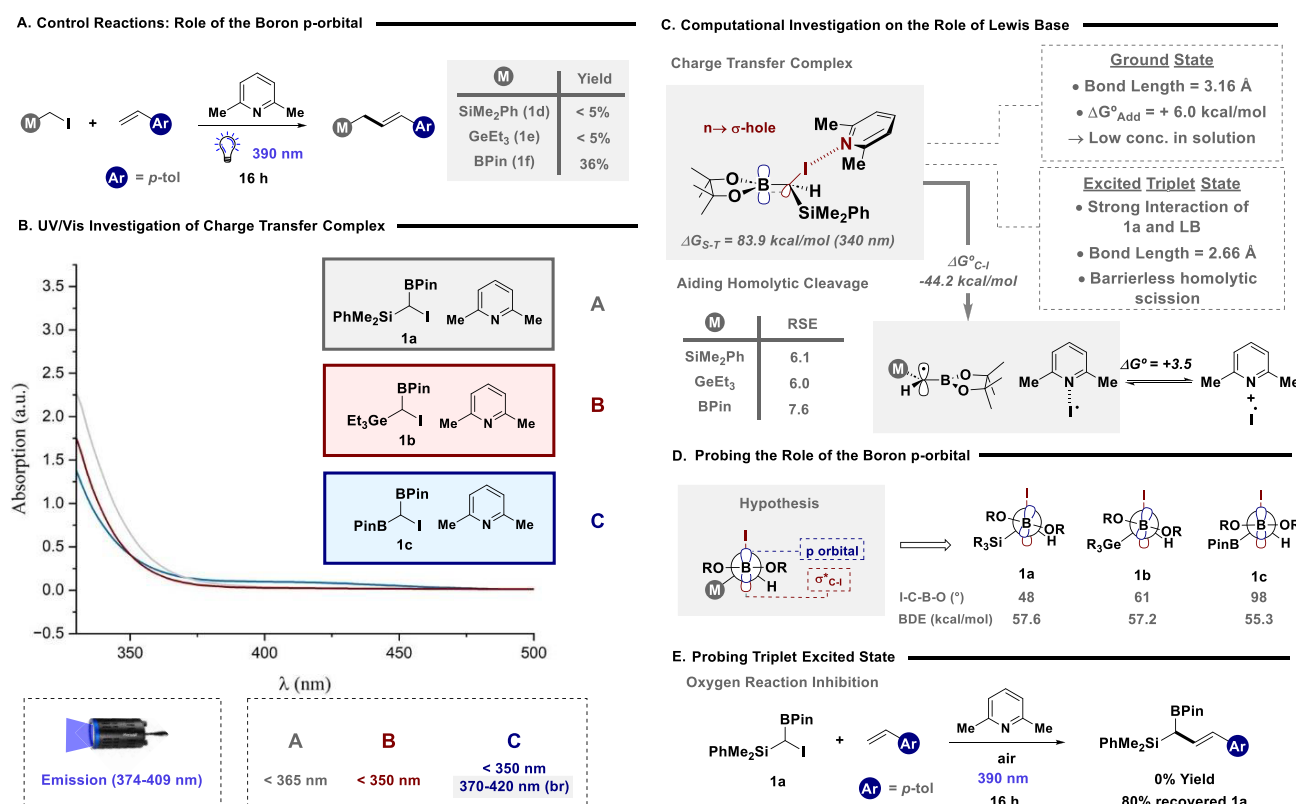


Figure 2. (A) Probing the role of the boron p-orbital for efficient reactivity. (B) UV/vis investigation on charge transfer complex formation. (C) Computational investigation on the role of the Lewis base. (D) Probing the role of the boron p-orbital. (E) Reaction inhibition by inclusion of oxygen.

leveraged as effective SOMOphiles to enable access to β -substituted ketones. Utilizing reagent **1a**, the reaction was tolerant of halides (**11**), enabling an additional handle for subsequent reactivity. Electron-neutral (**12**, **13**, and **15**), electron-poor (**14**), and electron-rich (**17**) silyl enol ethers were also tolerated in good yield. Intriguingly, aliphatic amines, typically prone to oxidation under photoredox reactivity,²⁶ were cleanly transformed to the target ketone (**16**). Alternative iodides **1b** and **1c** were also effective in engaging silyl enol ethers furnishing substrates **18–21** in moderate to good yield. The target reactivity was extended to diene SOMOphiles, to construct Diels–Alder compatible dienes containing boron and silicon as synthetic linchpins (**22** and **23**). The synthesis of oxindole derivatives (**24** and **25**) was achieved via a tandem process employing a phenyl-substituted acrylamide SOMOphile. Finally, the silyl enol ether derivative of iloperidone, a potent antipsychotic therapeutic,²⁷ was easily transformed to the corresponding ketone containing two boron handles for further downstream synthetic manipulations (**26**).

Given that the developed protocol mitigates the use of a photocatalyst or transition metal for efficient activation, we next set out to determine the *modus operandi* and key factors for the observed selective light-driven reactivity. As highlighted previously, the judicious choice of 2,6-lutidine was required for efficient reactivity, with alternative Lewis bases and inorganic bases proving ineffective (see ESI for full details). This is indicative that 2,6-lutidine, *inter alia*, is a key component for efficient radical generation. To probe our preliminary hypothesis that the trigonal planar boron p-orbital is also required, we assessed iodides without an adjacent boron substituent (Figure 2A). Utilizing α -silyl and α -germanyl

substrates **1d** and **1e** respectively led to no observed reactivity with complete retention of starting materials. However, employing the analogous α -boryl substituent, reactivity was restored underpinning the pivotal role of the boron p-orbital for efficient C–I bond activation. UV/vis analysis of ambiphilic starting materials (**1a–1c**), with solutions prepared in the dark at model reaction concentrations, determined that the precursors did not absorb the light of the incident Kessil lamp (see ESI for full details), while control reactions in the absence of additive (Table 1, entry 12) also support that efficient direct excitation of the reagents is not feasible. The inclusion of 2,6-lutidine led to a subtle alteration in absorption properties for both **1a** and **1b** leading to a small bathochromic shift (10 nm), while **1c** developed a broad band ranging from 370 to 420 nm (Figure 2B). An increase in concentration also led to a further bathochromic shift to longer wavelengths (10–20 nm; see ESI for full details). ¹H and ¹¹B NMR analysis of reaction components showed no notable sign of the previously envisioned halogen-bonding charge transfer complex and no dative interaction with the boron p-orbital to form a negatively charged boronate. However, when preparing solutions of both ambiphilic reagent and additive in the presence of light irradiation (390 nm, 20 min), small concentrations of triiodide were observed supporting light-induced homolytic cleavage of the C–I bond for all three precursors.²⁸ At this stage of the study, the origin of light-driven activation proved elusive and challenging to rationalize given that no clear precursor or intermediate was determined to be efficiently photoactive.

To interrogate the underlying origin of activation, a computational study of the model system was conducted at the SMD(MeCN) ω B97xD/def2TZVPP// ω B97xD/def2SVP

level of theory (Figure 2C). We initiated our study by probing the feasibility of halogen bonding between ambiphilic reagents **1a** and 2,6-lutidine in both the ground state and excited state (see the ESI for full details).

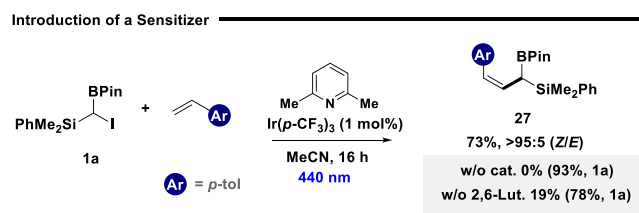
Pleasingly, the formation of an $n \rightarrow \sigma$ -hole charge transfer complex was shown to be energetically feasible with an estimated halogen bond length of 3.16 Å (see further details in the Supporting Information, Figures S36 and S37). We compare this interaction with the alternative formation of a boronate complex via the dative interaction of the Lewis base with the boron p-orbital. However, this interaction is not possible as the potential energy increases when the N center approximates the boron center (see ESI for full details). Predicted UV/vis of the charge transfer complex indicated that a new band with a bathochromic shift is generated, and the tail has significant overlap with the Kessil lamp at reaction concentration. However, with a relatively low NBO value for the σ -hole and an energy of formation established at 6.0 kcal/mol, it is foreseeable that a complex of this nature likely exists in low concentrations in solution, resulting in challenging detection by standard spectroscopic tools (UV/vis and NMR).²⁹

On translation to the triplet excited state, again a clear adduct between **1a** and 2,6-lutidine could be modeled with a shortened bond length of 2.66 Å. This structure shows a perpendicular interaction that comes from the partial C–I bond breaking, WBI (Wiberg Bond Index) = 0.2440, and N–I bond formation, WBI = 0.2045. Subsequent homolytic bond scission of the C–I bond in the triplet excited state was found to be highly energetically favored (–44.2 kcal/mol) through an almost barrierless conical intersection between the very close triplet electronic surfaces (<2 kcal/mol), estimated from the relaxed scan of the PES in both states (see ESI for full details). This generates comparatively stabilized α -bimetalloid radicals (RSE between 6.0 and 7.6 kcal/mol) and an iodine radical that is further stabilized by coordination to 2,6-lutidine (3.5 kcal/mol), due to the strong donor–acceptor interaction between the N lone pair and the partially occupied p orbital of iodine (WBI = 0.1627). These radical stabilities (RSE) are in sharp contrast to the more unstable **1d** and **1e** derived radicals (3.5 kcal/mol higher BDE). Having established the prominent role of 2,6-lutidine in both the activation of the C–I bond and the stabilization of the ensuing iodine radical, we next set out to unveil the pivotal role of the boron p-orbital. We initially envisaged that preferential alignment of the boron p-orbital and C–I antibonding orbital would result in a weakened bond and larger buildup of positive charge at the σ -hole at iodine, prompting interaction with a Lewis base.^{20a} While this was apparent for substrate **1c** (dihedral angle 98°, BDE 55.3 kcal/mol), the intrinsic electronic properties of **1a** and **1b** are not immediately clear, given the dihedral angles of 48° and 61° respectively. To gain a deeper insight, we analyzed the HOMO and LUMO structures of **1a** (see ESI). The HOMO is located on the lone pairs of iodine showing significant repulsion with both C–B and C–Si σ -bonds. However, analysis of the LUMO indicates that the C–I σ^* orbital is delocalized with both the p-orbital of boron and d-orbitals from silicon. It is anticipated that this delocalization again results in a weakened C–I bond and buildup of positive charge at the σ -hole. In summary, computational studies reveal that 2,6-lutidine plays a critical role in both the activation of ambiphilic reagents, through the formation of a photoactive halogen bonding charge transfer complex, and in the stabilization of transient iodine radicals.

The boron p-orbital was shown to influence the intrinsic properties of the C–I bond through orbital alignment and delocalization of the LUMO, creating a weakened bond for selective activation.

Our computational investigation supported the formation of a charge transfer complex in the triplet excited state (*vide supra*). In order to probe this reactivity we carried out reactions in the presence of oxygen a known triplet quencher (Figure 2E).³⁰ Under an oxygen atmosphere, reactivity was shown to be completely suppressed, leading to retention of the ambiphilic precursor **1a** in 80%. Inspired by this control reaction, we envisaged that the inclusion of an external photosensitizer may enable the reaction to be carried out efficiently at longer wavelengths (Scheme 2). However, on

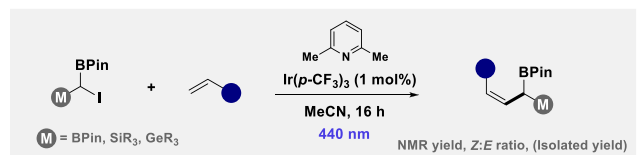
Scheme 2. Stereodivergent Synthesis of Z-Isomers



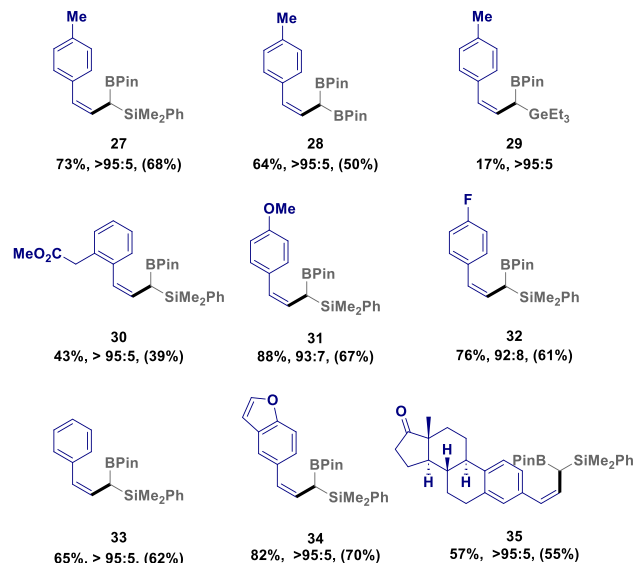
initially probing this reaction we found that activation also coincided with an energy transfer catalyzed geometric isomerization enabling the stereodivergent access to synthetically versatile Z-isomers (Scheme 2).^{31,32} Reaction optimization identified that the iridium catalyst Ir(p-CF₃)₃ could be used under 440 nm to enable expedient access to the corresponding Z-isomer (see ESI for full details). In the absence of 2,6-lutidine or the photocatalyst at 440 nm, reactivity was suppressed significantly, resulting in the retention of **1a**. These results highlight the importance of photocatalyst and additive for efficient reactivity also at 440 nm. It is pertinent to note that during reaction analysis no Ley-type photoredox activation of boron was observed providing further indication that 2,6-lutidine does not coordinate with the boron p-orbital.^{25b}

Catalyst screening identified that reactivity was contingent on excited state triplet energies and not on the photoredox properties of the excited state catalyst. However, while this is indicative of a sensitized process, energy transfer to charge transfer complexes is currently unknown, and direct homolytic activation of nonconjugated σ -bonds via energy transfer is, at present, limited to one synthetic example.³³ The model reaction conditions were compatible with ambiphilic reagent **1a** and a range of styrenes (Scheme 3), including electron-neutral (**27**, **30**, **33**, and **35**), electron-rich (**31**), electron-poor (**32**) and heterocyclic scaffolds (**34**). While ambiphilic reagent **1c** afforded the target Z-isomer (**28**) in good yield and selectivity, the use of germanium derivative **1b** was comparatively unsuccessful (**29**), again due to the competitive degradation of the formed product.

Guided by our mechanistic analysis thus far, we propose the following mode of activation and mechanistic hypothesis (Figure 3). It is proposed that an $n \rightarrow \sigma$ -hole interaction (A) between 2,6-lutidine and the ambiphilic reagent results in bond weakening and a bathochromic shift in absorption properties to aid efficient excitation (Figure 3, top).³⁴ Absorption of a photon is first envisaged to excite the adduct to the singlet excited state (B), where the heavy atom effect of iodine is

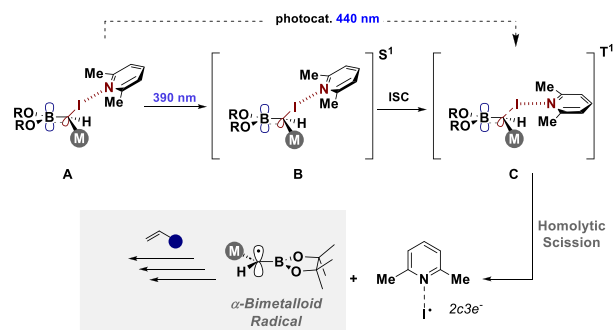
Scheme 3. Substrate Scope^a

Substrate Scope



^a(a) Reactions were performed in MeCN on a 0.2 mmol scale using 1 (1 equiv), SOMophile (3 equiv), 2,6-lutidine (1.5 equiv), and Ir(*p*-CF₃)₃ (1 mol %) under 440 nm irradiation (40 W). NMR yield and Z:E ratio were determined by ¹H NMR spectroscopy against a known internal standard (1,3,5-trimethoxybenzene).

Chemoselective Photoactivation of C–I Bond



Role of Stabilized Iodine Radical - Net Neutral Process

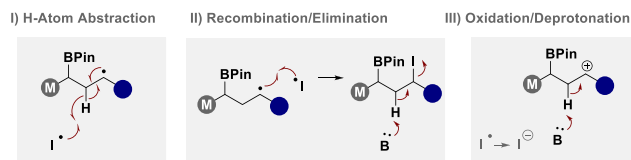


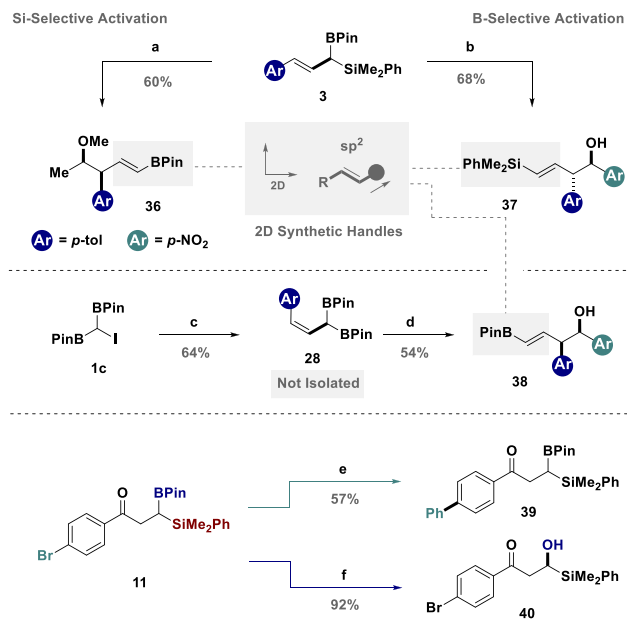
Figure 3. Proposed mechanism of activation.

predicted to enable facile inter-system crossing to the calculated triplet excited state (C).³⁵ Computational analysis then supports a barrierless homolytic scission of the C–I bond to form an α -bimetalloid radical primed for reactivity with a SOMophile and a stabilized iodine radical. While the quantum yield could not be determined accurately due to no clear overlap between incident light and absorbing intermediates,

light on/off experiments supported the absence of an efficient radical chain (see ESI for full details).³⁶ As a result, we propose the stabilized iodine radical serves to close the mechanism, resulting in a net neutral process. Contingent on employed SOMophile, this could occur via H-atom abstraction (Figure 3, bottom),³⁷ radical recombination and subsequent elimination, or oxidation followed by deprotonation.³⁸

The overarching vision of the study was to facilitate the light-driven, chemoselective activation of ambiphilic reagents to grant expedient access to organic scaffolds containing multiple synthetic handles that can permit the subsequent exploration of chemical space. To demonstrate the power of the methodology we next focused on product derivatization, paying particular attention to complimenting existing chemoselective activation modes (Figure 4).^{14a,39} Allylic system 3 containing both boron and silicon handles with orthogonal reactivity, was activated via a Hosomi–Sakurai reaction to grant access to vinyl BPin 36, as a single diastereomer, in good yield. Conventional allylation via activation of the boron motif enabled the synthesis of 37, containing a silicon handle for further derivitization. Complementary 3D vectors were

A. Chemoselective Activation of Products



B. Synthetic Utility of geminal-BPin

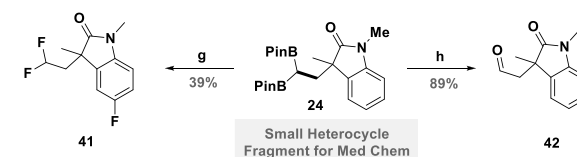


Figure 4. (A) Chemoselective activation of products: (a) 3, 1,1-dimethoxyethane (1.03 equiv), TiCl₄ (1.2 equiv), DCM, –78 °C; (b) 3, 4-nitrobenzaldehyde (1 equiv), MeCN, 50 °C; (c) 1c (1 equiv), 4-methylstyrene (3 equiv), 2–6-lutidine (1.5 equiv), MeCN, 390 nm irradiation; (d) 28, 4-nitrobenzaldehyde (1 equiv), MeCN, 50 °C; (e) 11 (1 equiv), phenylboronic acid (1.5 equiv), Pd(OAc)₂ (5 mol %), SPhos (10 mol %), K₃PO₄ (3 equiv), 1,4-dioxane, H₂O, 80 °C; (f) 11, NaBO₃·H₂O (3 equiv), THF, H₂O, 0 °C–rt; (B) synthetic utility of geminal-BPin: (g) 24 (1 equiv), AgNO₃ (0.2 equiv), selectfluor (3 equiv), TFA, H₃PO₄, H₂O, DCM, 50 °C; (h) 24 (1 equiv), NaBO₃·H₂O (3 equiv), THF, H₂O, 0 °C–rt.

accessed through the *Z*-allylic systems, with the allylation of **28** giving the *syn* vinyl BPin **38** in great diastereoselectivity. Aryl ketone **11** provided three orthogonal handles available for chemoselective transformations. This allowed selective activation of the aryl bromide through an sp²-selective Suzuki–Miyaura cross-coupling reaction to furnish biphenyl species **39**, while selective oxidation of the boron motif allowed for the formation of α -silyl alcohol **40**, which intriguingly avoided a Brooke rearrangement. In both of these examples, all other functional handles remained available for further downstream manipulations. Finally, geminal-BPin systems have been shown to be versatile precursors in synthesis, and to demonstrate their utility, oxindole fragment **24** was converted into the corresponding geminal difluoride (**41**),⁴⁰ a key motif in medicinal chemistry. Similarly, the translation of both boron motifs to a carbonyl was achieved in the synthesis of aldehyde **42**.⁴¹

CONCLUSIONS

In summary, we have developed an operationally simple chemoselective strategy to activate ambiphilic reagents to generate α -bimetalloid radicals using light and a simple Lewis base additive. These transient radicals can engage various SOMOphiles to grant expedient access to scaffolds containing multiple synthetic handles as 3D exit vectors. In-depth mechanistic and computational investigations revealed the prominent role of the boron p-orbital and 2,6-lutidine in the activation of the C–I bond via the formation of a halogen bonding charge transfer complex, while computational investigations also highlighted that photoactivated homolytic bond cleavage occurs in the triplet excited state, leading to the inception of a photocatalyzed stereodivergent approach to *Z*-isomers. The power of the method was demonstrated in product derivatization via chemoselective activation of pendant synthesis handles permitting the accurate exploration of chemical space. It is envisaged this mild platform to access high-energy α -bimetalloid radicals can be strategically paired with asymmetric cross-coupling protocols that will prove expansive as a future entry point into chiral hydrocarbons.⁴²

ASSOCIATED CONTENT

Supporting Information

The Supporting Information is available free of charge at <https://pubs.acs.org/doi/10.1021/jacs.4c02261>.

Experimental details, analytical data for compound characterization, reaction optimization, mechanistic studies, and computational studies (PDF)

AUTHOR INFORMATION

Corresponding Authors

Ignacio Funes-Ardoiz – Department of Chemistry, Instituto de Investigación Química de la Universidad de La Rioja (IQUR), Universidad de La Rioja Madre de Dios 53, Logroño 26004, Spain; orcid.org/0000-0002-5843-9660; Email: ignacio.funesa@unirioja.es

John J. Molloy – Department of Biomolecular Systems, Max-Planck-Institute of Colloids and Interfaces, Potsdam 14476, Germany; orcid.org/0000-0001-5337-0353; Email: john.molloy@mpikg.mpg.de

Authors

Lewis McGhie – Department of Biomolecular Systems, Max-Planck-Institute of Colloids and Interfaces, Potsdam 14476, Germany; Department of Chemistry and Biochemistry, Freie Universität Berlin, Berlin 14195, Germany

Alessandro Marotta – Department of Biomolecular Systems, Max-Planck-Institute of Colloids and Interfaces, Potsdam 14476, Germany; Department of Chemistry and Biochemistry, Freie Universität Berlin, Berlin 14195, Germany

Patrick O. Loftus – Department of Biomolecular Systems, Max-Planck-Institute of Colloids and Interfaces, Potsdam 14476, Germany

Peter H. Seeberger – Department of Biomolecular Systems, Max-Planck-Institute of Colloids and Interfaces, Potsdam 14476, Germany; Department of Chemistry and Biochemistry, Freie Universität Berlin, Berlin 14195, Germany; orcid.org/0000-0003-3394-8466

Complete contact information is available at: <https://pubs.acs.org/10.1021/jacs.4c02261>

Funding

Open access funded by Max Planck Society.

Notes

The authors declare no competing financial interest.

ACKNOWLEDGMENTS

We gratefully acknowledge financial support from the Max-Planck Society. A.M. and J.J.M. thank the Fonds der Chemischen Industrie, FCI for funding. P.O.L. and J.J.M. thank the Daimler and Benz Foundation for financial support. We thank the Mass Spec department of Freie Universität Berlin. I.F.-A. thanks the funding of PID2021-126075NB-I00 project and RYC2022-035776-I scholarship, funded by MCIN/AEI/10.13039/501100011033 and the European Union “Next Generation EU”/PRTR. We thank Layth Alama for preliminary experiments and Dr. Roza Bouchal for help with cyclic voltammetry experiments.

ABBREVIATIONS

BDE, bond dissociation energy; DCM, dichloromethane; DMF, dimethylformamide; ESI, electronic supporting information; HOMO, highest occupied molecular orbital; LUMO, lowest unoccupied molecular orbital; NMR, nuclear magnetic resonance; PES, potential energy surface; RSE, radical stabilization energy; SOMO, singly occupied molecular orbital; TFA, trifluoroacetic acid; UV, ultraviolet

REFERENCES

- (1) (a) Bleicher, K. H.; Böhm, H.-J.; Müller, K.; Alanine, A. I. Hit and Lead Generation: Beyond High-Throughput Screening. *Nat. Rev. Drug Discovery* **2003**, *2*, 369–378. (b) Boström, J.; Brown, D. G.; Young, R. J.; Keserü, G. M. Expanding the Medicinal Chemistry Synthetic Toolbox. *Nat. Rev. Drug Discovery* **2018**, *17*, 709–727. (c) Lombardino, J. G.; Lowe, J. A. The Role of the Medicinal Chemist in Drug Discovery — Then and Now. *Nat. Rev. Drug Discovery* **2004**, *3*, 853–862.
- (2) Reymond, J.-L. The Chemical Space Project. *Acc. Chem. Res.* **2015**, *48*, 722–730.
- (3) (a) Johansson Seechurn, C. C. C.; Kitching, M. O.; Colacot, T. J.; Snieckus, V. Palladium-Catalyzed Cross-Coupling: A Historical Contextual Perspective to the 2010 Nobel Prize. *Angew. Chem., Int. Ed.* **2012**, *51*, 5062–5085. (b) Lennox, A. J. J.; Lloyd-Jones, G. C.

Selection of Boron Reagents for Suzuki–Miyaura Coupling. *Chem. Soc. Rev.* **2014**, *43*, 412–443. (c) Denmark, S. E.; Sweis, R. F. Design and Implementation of New, Silicon-Based, Cross-Coupling Reactions: Importance of Silicon–Oxygen Bonds. *Acc. Chem. Res.* **2002**, *35*, 835–846. (d) Fyfe, J. W. B.; Watson, A. J. B. Recent Developments in Organoboron Chemistry: Old Dogs, New Tricks. *Chem* **2017**, *3*, 31–55.

(4) (a) Littke, A. F.; Dai, C.; Fu, G. C. Versatile Catalysts for the Suzuki Cross-Coupling of Arylboronic Acids with Aryl and Vinyl Halides and Triflates under Mild Conditions. *J. Am. Chem. Soc.* **2000**, *122*, 4020–4028. (b) Fairlamb, I. J. S. Regioselective (Site-Selective) Functionalisation of Unsaturated Halogenated Nitrogen, Oxygen and Sulfur Heterocycles by Pd-Catalyzed Cross-Couplings and Direct Arylation Processes. *Chem. Soc. Rev.* **2007**, *36*, 1036–1045. (c) Seath, C. P.; Fyfe, J. W. B.; Molloy, J. J.; Watson, A. J. B. Tandem Chemoselective Suzuki–Miyaura Cross-Coupling Enabled by Nucleophile Speciation Control. *Angew. Chem., Int. Ed.* **2015**, *54*, 9976–9979. (d) Kalvet, I.; Magnin, G.; Schoenebeck, F. Rapid Room-Temperature, Chemoselective C–C Coupling of Poly(Pseudo)-Halogenated Arenes Enabled by Palladium(I) Catalysis in Air. *Angew. Chem., Int. Ed.* **2017**, *56*, 1581–1585. (e) Keaveney, S. T.; Kundu, G.; Schoenebeck, F. Modular Functionalization of Arenes in a Triply Selective Sequence: Rapid C(Sp²) and C(Sp³) Coupling of C–Br, C–OTf, and C–Cl Bonds Enabled by a Single Palladium(I) Dimer. *Angew. Chem., Int. Ed.* **2018**, *57*, 12573–12577. (f) Diehl, C. J.; Scatolin, T.; Englert, U.; Schoenebeck, F. C–I-Selective Cross-Coupling Enabled by a Cationic Palladium Trimer. *Angew. Chem., Int. Ed.* **2019**, *58*, 211–215. (g) Norman, J. P.; Neufeldt, S. R. The Road Less Traveled: Unconventional Site Selectivity in Palladium-Catalyzed Cross-Couplings of Dihalogenated N-Heteroarenes. *ACS Catal.* **2022**, *12*, 12014–12026.

(5) (a) Dahiya, A.; Schoetz, M. D.; Schoenebeck, F. Orthogonal Olefination with Organogermanes. *Angew. Chem., Int. Ed.* **2023**, *62*, No. e202310380. (b) Bastick, K. A. C.; Watson, A. J. B. Pd-Catalyzed Organometallic-Free Homologation of Arylboronic Acids Enabled by Chemoselective Transmetalation. *ACS Catal.* **2023**, *13*, 7013–7018. (c) Fricke, C.; Schoenebeck, F. Organogermanes as Orthogonal Coupling Partners in Synthesis and Catalysis. *Acc. Chem. Res.* **2020**, *53*, 2715–2725.

(6) (a) Noguchi, H.; Hojo, K.; Sugimoto, M. Boron-Masking Strategy for the Selective Synthesis of Oligoarenes via Iterative Suzuki–Miyaura Coupling. *J. Am. Chem. Soc.* **2007**, *129*, 758–759. (b) Gillis, E. P.; Burke, M. D. A Simple and Modular Strategy for Small Molecule Synthesis: Iterative Suzuki–Miyaura Coupling of B-Protected Haloboronic Acid Building Blocks. *J. Am. Chem. Soc.* **2007**, *129*, 6716–6717. (c) Molander, G. A.; Sandrock, D. L. Orthogonal Reactivity in Boryl-Substituted Organotrifluoroborates. *J. Am. Chem. Soc.* **2008**, *130*, 15792–15793. (d) Lehmann, J. W.; Blair, D. J.; Burke, M. D. Towards the Generalized Iterative Synthesis of Small Molecules. *Nat. Rev. Chem.* **2018**, *2*, 0115. (e) Rygus, J. P. G.; Crudden, C. M. Enantiospecific and Iterative Suzuki–Miyaura Cross-Couplings. *J. Am. Chem. Soc.* **2017**, *139*, 18124–18137.

(7) (a) Li, J.; Ballmer, S. G.; Gillis, E. P.; Fujii, S.; Schmidt, M. J.; Palazzolo, A. M. E.; Lehmann, J. W.; Morehouse, G. F.; Burke, M. D. Synthesis of Many Different Types of Organic Small Molecules Using One Automated Process. *Science* **2015**, *347*, 1221–1226. (b) Blair, D. J.; Chitti, S.; Trobe, M.; Kostyra, D. M.; Haley, H. M. S.; Hansen, R. L.; Ballmer, S. G.; Woods, T. J.; Wang, W.; Mubayi, V.; Schmidt, M. J.; Pipal, R. W.; Morehouse, G. F.; Palazzolo Ray, A. M. E.; Gray, D. L.; Gill, A. L.; Burke, M. D. Automated Iterative Csp³–C Bond Formation. *Nature* **2022**, *604*, 92–97.

(8) Roughley, S. D.; Jordan, A. M. The Medicinal Chemist's Toolbox: An Analysis of Reactions Used in the Pursuit of Drug Candidates. *J. Med. Chem.* **2011**, *54*, 3451–3479.

(9) (a) Lovering, F.; Bikker, J.; Humblet, C. Escape from Flatland: Increasing Saturation as an Approach to Improving Clinical Success. *J. Med. Chem.* **2009**, *52*, 6752–6756. (b) Lovering, F. Escape from Flatland 2: Complexity and Promiscuity. *Medchemcomm* **2013**, *4*, 515–519. (c) Johnson, J. A.; Nicolaou, C. A.; Kirberger, S. E.;

Pandey, A. K.; Hu, H.; Pomerantz, W. C. K. Evaluating the Advantages of Using 3D-Enriched Fragments for Targeting BET Bromodomains. *ACS Med. Chem. Lett.* **2019**, *10*, 1648–1654.

(10) (a) Dostrovsky, I.; Hughes, E. D.; Ingold, C. K. 50. Mechanism of Substitution at a Saturated Carbon Atom. Part XXXII. The Role of Steric Hindrance. (Section G) Magnitude of Steric Effects, Range of Occurrence of Steric and Polar Effects, and Place of the Wagner Rearrangement in Nucleophilic Substitution and Elimination. *J. Chem. Soc.* **1946**, *0*, 173–194. (b) Ingold, C. K. Quantitative Study of Steric Hindrance. *Q. Rev. Chem. Soc.* **1957**, *11*, 1–14. (c) Xiang, J.; Shang, M.; Kawamata, Y.; Lundberg, H.; Reisberg, S. H.; Chen, M.; Mykhailiuk, P.; Beutner, G.; Collins, M. R.; Davies, A.; Del Bel, M.; Gallego, G. M.; Spangler, J. E.; Starr, J.; Yang, S.; Blackmond, D. G.; Baran, P. S. Hindered Dialkyl Ether Synthesis with Electrogenerated Carbocations. *Nature* **2019**, *573*, 398–402.

(11) (a) Matteson, D. S.; Majumdar, D. Deprotonation of a Trimethylsilylmethaneboronic Ester. *J. Chem. Soc. Chem. Commun.* **1980**, *1*, 39–40. (b) Matteson, D. S.; Majumdar, D. Alpha-Trimethylsilyl Boronic Esters Pinacol Lithio(Trimethylsilyl)-Methaneboronate, Homologation of Boronic Esters with [Chloro(Trimethylsilyl)methyl]Lithium, and Comparisons with Some Phosphorus and Sulfur Analogs. *Organometallics* **1983**, *2*, 230–236. (c) Tsai, D. J. S.; Matteson, D. S. Pinanediol [Alpha-(Trimethylsilyl)Allyl]Boronate and Related Boronic Esters. *Organometallics* **1983**, *2*, 236–241. (d) Aggarwal, V. K.; Binanzer, M.; de Ceglie, M. C.; Gallanti, M.; Glasspoole, B. W.; Kendrick, S. J. F.; Sonawane, R. P.; Vázquez-Romero, A.; Webster, M. P. Asymmetric Synthesis of Tertiary and Quaternary Allyl- and Crotylsilanes via the Borylation of Lithiated Carbamates. *Org. Lett.* **2011**, *13*, 1490–1493. (e) Millán, A.; Grigol Martínez, P. D.; Aggarwal, V. K. Stereocontrolled Synthesis of Polypropionate Fragments Based on a Building Block Assembly Strategy Using Lithiation-Borylation Methodologies. *Chem.—Eur. J.* **2018**, *24*, 730–735. (f) Bootwicha, T.; Feilner, J. M.; Myers, E. L.; Aggarwal, V. K. Iterative Assembly Line Synthesis of Polypropionates with Full Stereocontrol. *Nat. Chem.* **2017**, *9*, 896–902.

(12) (a) Hong, K.; Liu, X.; Morken, J. P. Simple Access to Elusive α -Boryl Carbanions and Their Alkylation: An Umpolung Construction for Organic Synthesis. *J. Am. Chem. Soc.* **2014**, *136*, 10581–10584. (b) Coombs, J. R.; Zhang, L.; Morken, J. P. Synthesis of Vinyl Boronates from Aldehydes by a Practical Boron–Wittig Reaction. *Org. Lett.* **2015**, *17*, 1708–1711. (c) Murray, S. A.; Liang, M. Z.; Meek, S. J. Stereoselective Tandem Bis-Electrophile Couplings of Diborylmethane. *J. Am. Chem. Soc.* **2017**, *139*, 14061–14064. (d) Murray, S. A.; Luc, E. C. M.; Meek, S. J. Synthesis of Alkenyl Boronates from Epoxides with Di-[B(Pin)]-Methane via Pd-Catalyzed Dehydroboration. *Org. Lett.* **2018**, *20*, 469–472. (e) Namirembe, S.; Gao, C.; Wexler, R. P.; Morken, J. P. Stereoselective Synthesis of Trisubstituted Alkenylboron Reagents by Boron-Wittig Reaction of Ketones. *Org. Lett.* **2019**, *21*, 4392–4394. (f) Cuenca, A. B.; Fernández, E. Boron-Wittig Olefination with Gem-Bis(Boryl)Alkanes. *Chem. Soc. Rev.* **2021**, *50*, 72–86. (g) Kim, H.; Jung, Y.; Cho, S. H. Defluorinative C–C Bond-Forming Reaction of Trifluoromethyl Alkenes with Gem-(Diborylalkyl)Lithiums. *Org. Lett.* **2022**, *24*, 2705–2710. (h) Han, S.; Lee, Y.; Jung, Y.; Cho, S. H. Stereoselective Access to Tetra- and Tri-Substituted Fluoro- and Chloro-Borylalkenes via Boron-Wittig Reaction. *Angew. Chem., Int. Ed.* **2022**, *61*, No. e202210532. (i) Kim, G.; Kim, M.; Ryu, C.; Choi, J.; Cho, S. H. Anion-Mediated, Stereospecific Synthesis of Secondary and Tertiary Cyclopropylboronates from Chiral Epoxides and Gem-Diborylalkanes. *Org. Lett.* **2023**, *25*, 4130–4134.

(13) (a) Lee, Y.; Han, S.; Cho, S. H. Catalytic Chemo- and Enantioselective Transformations of Gem-Diborylalkanes and (Diborylmethyl)Metallic Species. *Acc. Chem. Res.* **2021**, *54*, 3917–3929. (b) Palmer, W. N.; Obligation, J. V.; Pappas, I.; Chirik, P. J. Cobalt-Catalyzed Benzylic Borylation: Enabling Polyborylation and Functionalization of Remote, Unactivated C(Sp³)–H Bonds. *J. Am. Chem. Soc.* **2016**, *138*, 766–769. (c) Palmer, W. N.; Zarate, C.; Chirik, P. J. Benzyltriboronates: Building Blocks for Diastereoselective

Carbon–Carbon Bond Formation. *J. Am. Chem. Soc.* **2017**, *139*, 2589–2592. (d) Lee, Y.; Park, J.; Cho, S. H. Generation and Application of (Diborylmethyl)Zinc(II) Species: Access to Enantioenriched Gem-Diborylalkanes by an Asymmetric Allylic Substitution. *Angew. Chem., Int. Ed.* **2018**, *57*, 12930–12934. (e) Kim, J.; Cho, S. H. Access to Enantioenriched Benzylic 1,1-Silylboronate Esters by Palladium-Catalyzed Enantiotopic-Group Selective Suzuki–Miyaura Coupling of (Diborylmethyl)Silanes with Aryl Iodides. *ACS Catal.* **2019**, *9*, 230–235. (f) Lee, H.; Lee, Y.; Cho, S. H. Palladium-Catalyzed Chemoselective Negishi Cross-Coupling of Bis-[(Pinacolato)Boryl]Methylzinc Halides with Aryl (Pseudo)Halides. *Org. Lett.* **2019**, *21*, 5912–5916. (g) Kim, J.; Lee, E.; Cho, S. H. Chemoselective Palladium-Catalyzed Suzuki–Miyaura Cross-Coupling of (Diborylmethyl)Silanes with Alkenyl Bromides. *Asian J. Org. Chem.* **2019**, *8*, 1664–1667.

(14) (a) Selmani, A.; Schoetz, M. D.; Queen, A. E.; Schoenebeck, F. Modularity in the Csp^3 Space—Alkyl Germanes as Orthogonal Molecular Handles for Chemoselective Diversification. *ACS Catal.* **2022**, *12*, 4833–4839. (b) Shimizu, M.; Kurahashi, T.; Kitagawa, H.; Shimono, K.; Hiyma, T. Gem-Silylborylation Approach for Tri- and Tetramethylmethanes: The First Synthesis of Boryl(Germyl)(Silyl)-(Stannyl)Methanes. *J. Organomet. Chem.* **2003**, *686*, 286–293. (c) Kurandina, D.; Parasram, M.; Gevorgyan, V. Visible Light-Induced Room-Temperature Heck Reaction of Functionalized Alkyl Halides with Vinyl Arenes/Heteroarenes. *Angew. Chem., Int. Ed.* **2017**, *56*, 14212–14216. (d) Benoit, G.; Charette, A. B. Diastereoselective Borocyclopropanation of Allylic Ethers Using a Boromethylzinc Carbenoid. *J. Am. Chem. Soc.* **2017**, *139*, 1364–1367.

(15) (a) Hwang, C.; Lee, Y.; Kim, M.; Seo, Y.; Cho, S. H. Diborylmethyl Group as a Transformable Building Block for the Diversification of Nitrogen-Containing Molecules. *Angew. Chem., Int. Ed.* **2022**, *61*, No. e202209079. (b) Kondo, J.; Shinokubo, H.; Oshima, K. Oxidation of Gem-Borylsilylalkylcoppers to Acylsilanes with Air. *Org. Lett.* **2006**, *8*, 1185–1187.

(16) (a) Sayes, M.; Benoit, G.; Charette, A. B. Borocyclopropanation of Styrenes Mediated by UV-Light Under Continuous Flow Conditions. *Angew. Chem., Int. Ed.* **2018**, *57*, 13514–13518. (b) Thai-Savard, L.; Sayes, M.; Perreault-Dufour, J.; Hong, G.; Wells, L. A.; Kozlowski, M. C.; Charette, A. B. Organocatalyzed Visible Light-Mediated Gem-Borosilylcyclopropanation. *J. Org. Chem.* **2023**, *88*, 1515–1521. (c) Hu, J.; Tang, M.; Wang, J.; Wu, Z.; Friedrich, A.; Marder, T. B. Photocatalyzed Borylcyclopropanation of Alkenes with a (Diborylmethyl)Iodide Reagent. *Angew. Chem., Int. Ed.* **2023**, *62*, No. e202305175.

(17) Marotta, A.; Adams, C. E.; Molloy, J. J. The Impact of Boron Hybridisation on Photocatalytic Processes. *Angew. Chem., Int. Ed.* **2022**, *61*, No. e202207067.

(18) For reviews on the generation of α -boryl radicals see: (a) Kumar, N.; Reddy, R. R.; Eghbarieh, N.; Masarwa, A. α -Borylalkyl Radicals: Their Distinctive Reactivity in Modern Organic Synthesis. *Chem. Commun.* **2020**, *56*, 13–25. (b) Lovinger, G. J.; Morken, J. P. Recent Advances in Radical Addition to Alkenylboron Compounds. *Eur. J. Org. Chem.* **2020**, *2020*, 2362–2368. (c) Kischkewitz, M.; Friese, F. W.; Studer, A. Radical-Induced 1,2-Migrations of Boron Ate Complexes. *Adv. Synth. Catal.* **2020**, *362*, 2077–2087.

(19) For selected examples on the generation of α -boryl radicals see: (a) Kischkewitz, M.; Okamoto, K.; Mück-Lichtenfeld, C.; Studer, A. Radical-Polar Crossover Reactions of Vinylboron Ate Complexes. *Science* **2017**, *355*, 936–938. (b) Silvi, M.; Sandford, C.; Aggarwal, V. K. Merging Photoredox with 1,2-Metallate Rearrangements: The Photochemical Alkylation of Vinyl Boronate Complexes. *J. Am. Chem. Soc.* **2017**, *139*, 5736–5739. (c) Gerleve, C.; Kischkewitz, M.; Studer, A. Synthesis of α -Chiral Ketones and Chiral Alkanes Using Radical Polar Crossover Reactions of Vinyl Boron Ate Complexes. *Angew. Chem., Int. Ed.* **2018**, *57*, 2441–2444. (d) Kischkewitz, M.; Gerleve, C.; Studer, A. Radical-Polar Crossover Reactions of Dienylboronate Complexes: Synthesis of Functionalized Allylboronic Esters. *Org. Lett.* **2018**, *20*, 3666–3669. (e) Silvi, M.; Aggarwal, V. K. Radical Addition to Strained σ -Bonds Enables the Sterecontrolled Synthesis of

Cyclobutyl Boronic Esters. *J. Am. Chem. Soc.* **2019**, *141*, 9511–9515. (f) Noble, A.; Mega, R. S.; Pflästerer, D.; Myers, E. L.; Aggarwal, V. K. Visible-Light-Mediated Decarboxylative Radical Additions to Vinyl Boronic Esters: Rapid Access to γ -Amino Boronic Esters. *Angew. Chem., Int. Ed.* **2018**, *57*, 2155–2159. (g) Nagaraju, A.; Saiaede, T.; Eghbarieh, N.; Masarwa, A. Photoredox-Mediated Deoxygenative Radical Additions of Aromatic Acids to Vinyl Boronic Esters and Gem-Diborylalkenes. *Chem.—Eur. J.* **2023**, *29*, No. e202202646. (h) Kumar, N.; Eghbarieh, N.; Stein, T.; Shames, A. I.; Masarwa, A. Photoredox-Mediated Reaction of Gem-Diborylalkenes: Reactivity Toward Diverse 1,1-Bisborylalkanes. *Chem.—Eur. J.* **2020**, *26*, 5360–5364. (i) Marotta, A.; Fang, H.; Adams, C. E.; Sun Marcus, K.; Daniliuc, C. G.; Molloy, J. J. Direct Light-Enabled Access to α -Boryl Radicals: Application in the Stereodivergent Synthesis of Allyl Boronic Esters. *Angew. Chem., Int. Ed.* **2023**, *62*, No. e202307540.

(20) For reviews see: (a) Crisenza, G. E. M.; Mazzarella, D.; Melchiorre, P. Synthetic Methods Driven by the Photoactivity of Electron Donor–Acceptor Complexes. *J. Am. Chem. Soc.* **2020**, *142*, 5461–5476. (b) Piedra, H. F.; Valdés, C.; Plaza, M. Shining Light on Halogen-Bonding Complexes: A Catalyst-Free Activation Mode of Carbon–Halogen Bonds for the Generation of Carbon-Centered Radicals. *Chem. Sci.* **2023**, *14*, 5545–5568. (c) Sutar, R. L.; Huber, S. M. Catalysis of Organic Reactions through Halogen Bonding. *ACS Catal.* **2019**, *9*, 9622–9639.

(21) For selected examples see: (a) Matsuo, K.; Kondo, T.; Yamaguchi, E.; Itoh, A. Photoinduced Atom Transfer Radical Addition Reaction of Olefins with α -Bromo Carbonyls. *Chem. Pharm. Bull.* **2021**, *69*, 796–801. (b) Fuks, E.; Huber, L.; Schinkel, T.; Trapp, O. Investigation of Straightforward, Photoinduced Alkylations of Electron-Rich Heterocompounds with Electron-Deficient Alkyl Bromides in the Sole Presence of 2,6-Lutidine. *Eur. J. Org. Chem.* **2020**, *2020*, 6192–6198. (c) Kato, N.; Nanjo, T.; Takemoto, Y. A Pyridine-Based Donor–Acceptor Molecule: A Highly Reactive Organophotocatalyst That Enables the Reductive Cleavage of C–Br Bonds through Halogen Bonding. *ACS Catal.* **2022**, *12*, 7843–7849. (d) Treacy, S. M.; Vaz, D. R.; Noman, S.; Tard, C.; Rovis, T. Coupling of α -Bromoamides and Unactivated Alkenes to Form γ -Lactams through EDA and Photocatalysis. *Chem. Sci.* **2023**, *14*, 1569–1574.

(22) Crespi, S.; Fagnoni, M. Generation of Alkyl Radicals: From the Tyranny of Tin to the Photon Democracy. *Chem. Rev.* **2020**, *120*, 9790–9833.

(23) For pyridine derived stabilization of halide radicals see: (a) Breslow, R.; Brandl, M.; Hunger, J.; Turro, N.; Cassidy, K.; Krogh-Jespersen, K.; Westbrook, J. D. Pyridine Complexes of Chlorine Atoms. *J. Am. Chem. Soc.* **1987**, *109*, 7204–7206. (b) Rohe, S.; Morris, A. O.; McCallum, T.; Barriault, L. Hydrogen Atom Transfer Reactions via Photoredox Catalyzed Chlorine Atom Generation. *Angew. Chem., Int. Ed.* **2018**, *57*, 15664–15669.

(24) For the comparative stabilization of halide radicals see: (a) Isse, A. A.; Lin, C. Y.; Coote, M. L.; Gennaro, A. Estimation of Standard Reduction Potentials of Halogen Atoms and Alkyl Halides. *J. Phys. Chem. B* **2011**, *115*, 678–684. (b) Shen, Y.; Gu, Y.; Martin, R. Sp³ C–H Arylation and Alkylation Enabled by the Synergy of Triplet Excited Ketones and Nickel Catalysts. *J. Am. Chem. Soc.* **2018**, *140*, 12200–12209. (c) Bonciolini, S.; Noël, T.; Capaldo, L. Synthetic Applications of Photocatalyzed Halogen-Radical Mediated Hydrogen Atom Transfer for C–H Bond Functionalization. *Eur. J. Org. Chem.* **2022**, *2022*, No. e202200417.

(25) (a) Cox, P. A.; Leach, A. G.; Campbell, A. D.; Lloyd-Jones, G. C. Protodeboronation of Heteroaromatic, Vinyl, and Cyclopropyl Boronic Acids: PH–Rate Profiles, Autocatalysis, and Disproportionation. *J. Am. Chem. Soc.* **2016**, *138*, 9145–9157. (b) Lima, F.; Sharma, U. K.; Grunenberg, L.; Saha, D.; Johannsen, S.; Sedelmeier, J.; Van der Eycken, E. V.; Ley, S. V. A Lewis Base Catalysis Approach for the Photoredox Activation of Boronic Acids and Esters. *Angew. Chem., Int. Ed.* **2017**, *56*, 15136–15140. (c) Pillitteri, S.; Ranjan, P.; Van der Eycken, E. V.; Sharma, U. K. Uncovering the Potential of

Boronic Acid and Derivatives as Radical Source in Photo(Electro)-Chemical Reactions. *Adv. Synth. Catal.* **2022**, *364*, 1643–1665.

(26) Constantin, T.; Zanini, M.; Regni, A.; Sheikh, N. S.; Juliá, F.; Leonori, D. Aminoalkyl Radicals as Halogen-Atom Transfer Agents for Activation of Alkyl and Aryl Halides. *Science* **2020**, *367*, 1021–1026.

(27) Citrome, L. Iloperidone for Schizophrenia: A Review of the Efficacy and Safety Profile for This Newly Commercialised Second-Generation Antipsychotic. *Int. J. Clin. Pract.* **2009**, *63*, 1237–1248.

(28) Pursell, J. L.; Pursell, C. J. Host–Guest Inclusion Complexation of α -Cyclodextrin and Triiodide Examined Using UV–Vis Spectrophotometry. *J. Phys. Chem. A* **2016**, *120*, 2144–2149.

(29) Zhao, G.; Lim, S.; Musaev, D. G.; Ngai, M.-Y. Expanding Reaction Profile of Allyl Carboxylates via 1,2-Radical Migration (RaM): Visible-Light-Induced Phosphine-Catalyzed 1,3-Carbobromination of Allyl Carboxylates. *J. Am. Chem. Soc.* **2023**, *145*, 8275–8284.

(30) Grewer, C.; Brauer, H.-D. Mechanism of the Triplet-State Quenching by Molecular Oxygen in Solution. *J. Phys. Chem.* **1994**, *98*, 4230–4235.

(31) For reviews see: (a) Pearson, C. M.; Snaddon, T. N. Alkene Photo-Isomerization Inspired by Vision. *ACS Cent. Sci.* **2017**, *3*, 922–924. (b) Molloy, J. J.; Morack, T.; Gilmour, R. Positional and Geometrical Isomerisation of Alkenes: The Pinnacle of Atom Economy. *Angew. Chem., Int. Ed.* **2019**, *58*, 13654–13664.

(c) Nevešely, T.; Wienhold, M.; Molloy, J. J.; Gilmour, R. Advances in the $E \rightarrow Z$ Isomerization of Alkenes Using Small Molecule Photocatalysts. *Chem. Rev.* **2022**, *122*, 2650–2694.

(32) For selected examples containing cross-coupling nucleophiles see: (a) Molloy, J. J.; Metternich, J. B.; Daniliuc, C. G.; Watson, A. J. B.; Gilmour, R. Contra-Thermodynamic, Photocatalytic $E \rightarrow Z$ Isomerization of Styrenyl Boron Species: Vectors to Facilitate Exploration of Two-Dimensional Chemical Space. *Angew. Chem., Int. Ed.* **2018**, *57*, 3168–3172. (b) Faßbender, S. I.; Molloy, J. J.; Mück-Lichtenfeld, C.; Gilmour, R. Geometric $E \rightarrow Z$ Isomerisation of Alkenyl Silanes by Selective Energy Transfer Catalysis: Stereodivergent Synthesis of Triarylethylenes via a Formal Anti-Metallo-metallation. *Angew. Chem., Int. Ed.* **2019**, *58*, 18619–18626. (c) Molloy, J. J.; Schäfer, M.; Wienhold, M.; Morack, T.; Daniliuc, C. G.; Gilmour, R. Boron-Enabled Geometric Isomerization of Alkenes via Selective Energy-Transfer Catalysis. *Science* **2020**, *369*, 302–306. (d) Brégent, T.; Bouillon, J.-P.; Poisson, T. Photocatalyzed $E \rightarrow Z$ Contra-Thermodynamic Isomerization of Vinyl Boronates with Binaphthol. *Chem. – Eur. J.* **2021**, *27*, 13966–13970. (e) Fan, Q.; Huang, J.; Lin, S.; Chen, Z.-H.; Li, Q.; Yin, B.; Wang, H. Catalyst-Enabled Stereodivergence in Photochemical Atom Transfer Radical Addition (ATRA) of α -Iodoboronic Esters to Alkynes. *ACS Catal.* **2024**, *14*, 299–307.

(33) Teders, M.; Henkel, C.; Anhäuser, L.; Strieth-Kalthoff, F.; Gómez-Suárez, A.; Kleinmans, R.; Kahnt, A.; Rentmeister, A.; Guldi, D.; Glorius, F. The Energy-Transfer-Enabled Biocompatible Disulfide–Ene Reaction. *Nat. Chem.* **2018**, *10*, 981–988.

(34) Additional aggregation effects caused by solvent and reaction media can also be beneficial for reactivity. For reviews see: (a) Sempere, Y.; Morgenstern, M.; Bach, T.; Plaza, M. Reactivity and Selectivity Modulation within a Molecular Assembly: Recent Examples from Photochemistry. *Photochem. Photobiol. Sci.* **2022**, *21*, 719–737. (b) Mandigma, M. J. P.; Kaur, J.; Barham, J. P. Organophotocatalytic Mechanisms: Simplicity or Naivety? Diverting Reactive Pathways by Modifications of Catalyst Structure, Redox States and Substrate Preassemblies. *ChemCatChem* **2023**, *15*, No. e202201542.

(35) (a) Koziar, J. C.; Cowan, D. O. Photochemical Heavy-Atom Effects. *Acc. Chem. Res.* **1978**, *11*, 334–341. (b) Rey, Y. P.; Abradelo, D. G.; Santschi, N.; Strassert, C. A.; Gilmour, R. Quantitative Profiling of the Heavy-Atom Effect in BODIPY Dyes: Correlating Initial Rates, Atomic Numbers, and IO₂ Quantum Yields. *Eur. J. Org. Chem.* **2017**, *2017*, 2170–2178. (c) Marian, C. M. Understanding and Controlling Intersystem Crossing in Molecules. *Annu. Rev. Phys. Chem.* **2021**, *72*, 617–640. (d) Doležel, J.; Poryvai, A.; Slanina, T.; Filgas, J.; Slavíček,

P. Spin-Vibronic Coupling Controls the Intersystem Crossing of Iodine-Substituted BODIPY Triplet Chromophores. *Chem.—Eur. J.* **2024**, *30*, No. e202303154.

(36) Light on/off experiments cannot comprehensively rule out radical chain mechanisms with short propagations.; Cismesia, M. A.; Yoon, T. P. Characterizing Chain Processes in Visible Light Photoredox Catalysis. *Chem. Sci.* **2015**, *6*, 5426–5434.

(37) Chen, K.-Q.; Shen, J.; Wang, Z.-X.; Chen, X.-Y. A Donor–Acceptor Complex Enables the Synthesis of E-Olefins from Alcohols, Amines and Carboxylic Acids. *Chem. Sci.* **2021**, *12*, 6684–6690.

(38) Lewis-Borrell, L.; Sneha, M.; Clark, I. P.; Fasano, V.; Noble, A.; Aggarwal, V. K.; Orr-Ewing, A. J. Direct Observation of Reactive Intermediates by Time-Resolved Spectroscopy Unravels the Mechanism of a Radical-Induced 1,2-Metalate Rearrangement. *J. Am. Chem. Soc.* **2021**, *143*, 17191–17199.

(39) For reviews please see: (a) Nallagonda, R.; Padala, K.; Masarwa, A. Gem-Diborylalkanes: Recent Advances in Their Preparation. *Transformation and Application. Org. Biomol. Chem.* **2018**, *16*, 1050–1064. (b) Kranidiotis-Hisatomi, N.; Oestreich, M. Advances in Enantioconvergent Transition-Metal-Catalyzed Cross-Coupling Reactions of Racemic α -Silyl and α -Boryl Reagents. *Synthesis* **2023**, *55*, 1497–1506. (c) Zhang, C.; Hu, W.; Morken, J. P. α -Boryl Organometallic Reagents in Catalytic Asymmetric Synthesis. *ACS Catal.* **2021**, *11*, 10660–10680. For selected examples please see: (d) Lee, J. C. H.; McDonald, R.; Hall, D. G. Enantioselective Preparation and Chemoselective Cross-Coupling of 1,1-Diboron Compounds. *Nat. Chem.* **2011**, *3*, 894–899. (e) Sun, C.; Potter, B.; Morken, J. P. A Catalytic Enantiotopic-Group-Selective Suzuki Reaction for the Construction of Chiral Organoboronates. *J. Am. Chem. Soc.* **2014**, *136*, 6534–6537. (f) Sun, H.-Y.; Kubota, K.; Hall, D. G. Reaction Optimization, Scalability, and Mechanistic Insight on the Catalytic Enantioselective Desymmetrization of 1,1-Diborylalkanes via Suzuki–Miyaura Cross-Coupling. *Chem.—Eur. J.* **2015**, *21*, 19186–19194. (g) Joannou, M. V.; Moyer, B. S.; Meek, S. J. Enantio- and Diastereoselective Synthesis of 1,2-Hydroxyboronates through Cu-Catalyzed Additions of Alkylboronates to Aldehydes. *J. Am. Chem. Soc.* **2015**, *137*, 6176–6179. (h) Szymaniak, A. A.; Zhang, C.; Coombs, J. R.; Morken, J. P. Enantioselective Synthesis of Nonracemic Geminal Silylboronates by Pt-Catalyzed Hydrosilylation. *ACS Catal.* **2018**, *8*, 2897–2901. (i) Kumar, N.; Reddy, R. R.; Masarwa, A. Stereoselective Desymmetrization of Gem-Diborylalkanes by “Trifluorination. *Chem.—Eur. J.* **2019**, *25*, 8008–8012. (j) Park, J.; Jung, Y.; Kim, J.; Lee, E.; Lee, S. Y.; Cho, S. H. Kinetic Resolution of α -Silyl-Substituted Allylboronate Esters via Chemo- and Stereoselective Allylboration of Aldehydes. *Adv. Synth. Catal.* **2021**, *363*, 2371–2376. (k) Kong, Z.; Hu, W.; Morken, J. P. 1,2-Diborylsilanes: Catalytic Enantioselective Synthesis and Site-Selective Cross-Coupling. *ACS Catal.* **2023**, *13*, 11522–11527.

(40) Li, Z.; Wang, Z.; Zhu, L.; Tan, X.; Li, C. Silver-Catalyzed Radical Fluorination of Alkylboronates in Aqueous Solution. *J. Am. Chem. Soc.* **2014**, *136*, 16439–16443.

(41) Wu, C.; Wang, J. Geminal Bis(Boron) Compounds: Their Preparation and Synthetic Applications. *Tetrahedron Lett.* **2018**, *59*, 2128–2140.

(42) Saito, F.; Schreiner, P. R. Determination of the Absolute Configurations of Chiral Alkanes – An Analysis of the Available Tools. *Eur. J. Org. Chem.* **2020**, *2020*, 6328–6339.